

## ORIGINAL ARTICLE

### Real space flight travel is associated with ultrastructural changes, cytoskeletal disruption and premature senescence of HUVEC

MY KAPITONOVA MD, PhD, S MUID\* BSc, MSc, GRA FROEMMING MSc, PhD, WNW YUSOFF\* BSc, S Othman BSc, AM Ali\*\* MSc, PhD, and HM NAWAWI\* MRCPath, FRCPath

*Institute of Medical Molecular Biotechnology (IMMB), \*The Centre for Pathology Diagnostic and Research Laboratories (CPDRL), Faculty of Medicine, Universiti Teknologi MARA, Malaysia and \*\*Faculty of Agriculture and Biotechnology, Universiti Sultan Zainal Abidin, Terengganu, Malaysia*

#### Abstract

Microgravity, hypergravity, vibration, ionizing radiation and temperature fluctuations are major factors of outer space flight affecting human organs and tissues. There are several reports on the effect of space flight on different human cell types of mesenchymal origin while information regarding changes to vascular endothelial cells is scarce.

Ultrastructural and cytophysiological features of macrovascular endothelial cells in outer space flight and their persistence during subsequent culturing were demonstrated in the present investigation. At the end of the space flight, endothelial cells displayed profound changes indicating cytoskeletal lesions and increased cell membrane permeability. Readapted cells of subsequent passages exhibited persisting cytoskeletal changes, decreased metabolism and cell growth indicating cellular senescence.

**Keywords:** endothelium, microgravity, cell growth, cytoskeleton, senescence

#### INTRODUCTION

Over the past fifty years since the 1<sup>st</sup> manned orbital outer space flight by Y.A. Gagarin, the effects of microgravity, radiation, vibration and other factors affecting human body cells and tissues during piloted outer space flight have been investigated by many scientists. Most of the research was performed using simulated microgravity and other conditions associated with space flight.<sup>1-6</sup> Real space flight is more reflective of real life situations where microgravity is combined with other factors that include vibration, hypergravity, mechanical stress and radiation. However there are few studies on the responses of human and animal cell cultures to actual space flight conditions.<sup>7-10</sup> Recently, there has been intensified research interest in space science, particularly with the emergence of new space programs such as MARS100 and MARS500. The daring plans of earth inhabitants to fly to other planets may impose a challenging load on the cells and tissues of human beings. As satisfactory strategies are still unclear

with regards to bone loss prevention, vascular alterations and other space flight-related lesions, more research is required on the mechanisms of the effect of space flight on the structure and function of human cells, including endothelium which is one of the tissues most sensitive to space flight conditions.

Endothelial cells form the inner lining of blood vessels and play a crucial role in maintaining the functional integrity of the vascular wall. Various insults including inflammation and oxidative stress lead to endothelial dysfunction, an early event in atherosclerosis.<sup>11</sup> However, the effect of microgravity and other space flight-related conditions on in-vitro endothelial cells is still unclear.<sup>6</sup> Given that space flight conditions may possibly lead to endothelial dysfunction, which is pivotal in the pathogenesis of atherosclerosis, it is important to study the effect of space travel on live endothelial cells.

The objective of the present investigation was to examine the effect of short space flight on the morphology and growth rate of human umbilical

*Address for correspondence and reprint requests:* Prof Dr Hapizah Mohd Nawawi, The Centre for Pathology Diagnostic and Research Laboratories (CPDRL), Faculty of Medicine, Universiti Teknologi MARA, Jalan Hospital, 47000 Sungai Buloh, Selangor, Malaysia. e-mail: hapizah.nawawi@gmail.com

vein endothelial cells (HUVEC) as a model for endothelial function *in vitro*.

## MATERIALS AND METHODS

Fluid processing apparatus (FPA) were obtained from Bioserve, USA. Medium 200 and low serum growth supplements (LSGS) were obtained from Cascade Biologics, USA. Accutase was purchased from ICN Biomedical, USA. Cytodex-3 microcarrier beads were purchased from GE Healthcare Biosciences AB, Sweden. Phosphate buffered saline (PBS) was obtained from MP Biomedicals, France. Quantigene Plex 2 assay kit was purchased from Panomics, USA. Paraformaldehyde and osmium tetroxide were purchased from Sigma Aldrich, USA. MitoTracker® red, Hoechst 33342 and Tubulin Tracker™ green staining dyes were manufactured by Invitrogen, USA. Trypan blue solution was purchased from Gibco, USA.

### *Cell culture*

HUVEC line was purchased from Cascade Biologics, USA. HUVEC were cultured in medium 200 supplemented with LSGS in a humidified incubator set at 37°C and 5% carbon dioxide (CO<sub>2</sub>) until confluent. The split ratio was 1:2. Prior to the addition of HUVEC into FPA, HUVEC at passage 4 were cultured onto a microcarrier (Cytodex 3) in Petri dishes and incubated at 37°C in a 5% CO<sub>2</sub> incubator for 24 hours. This timeline was sufficient to allow HUVEC to attach to the microcarrier surface.

Details of the Soyuz TMA-11 12-day outer space flight were as follows: launch on October 10, 2007; landing on October 21, 2007; flight code: 2007-045A/32256. ISS location was maintained at an orbit between 278 and 460 km altitude. This particular experiment was conducted in the Russian Segment of the ISS.

Two days prior to the launch of the Soyuz TMA-11, the cells were loaded into 2 sets of FPA, each in duplicate. Each FPA consists of 3 chambers: A, B and C. Two sets of FPA were prepared to accommodate scanning electron microscopy (SEM) analysis of immediate postflight (IPF) samples and revived HUVEC (RAP). The cells were loaded in chamber A, additional culture medium in chamber B and 4% paraformaldehyde (for SEM analysis) or culture medium (for RAP) in chamber C. Then, the FPAs were incubated at 37°C in the 5% CO<sub>2</sub> incubator. They were handed over to the engineers at 12 hours before launch to be

placed in Soyuz TMA-11. During launch and up to docking, the FPAs containing the HUVEC were stowed at ambient temperature (18-22°C) in the Nomex bag. On the day L+4 (4 days after launch), the fresh culture medium from chamber B was added into Chamber A of both sets of FPA. The FPAs were placed back in the Kubik Amber incubator at 37°C. At -8 hours before undocking, FPAs were taken out to perform the termination process. Fixative (4% paraformaldehyde) or culture medium was added into the cells. FPAs were then packed into a Nomex Bag (CIS kit) and transferred to the Soyuz capsule for return to earth. The temperature profile was recorded by HOBO which was placed in the Nomex bag. Upon landing, the FPAs were kept in a 4°C thermo-container and transported to the laboratory. Cells in 4% paraformaldehyde were collected and stored at 4°C until analysis.

### *SEM analysis of immediate post-flight cells (IPF)*

Asynchronous ground controls were performed as a control for IPF samples using the spaceflight temperature profile according to the HOBO reader. The actual temperature ground controls (ATGC) were performed to control for the effects of temperature fluctuations occurring throughout the space mission as stated in Table 1. In addition, they were controlled for initial cell density, type of culture medium, growth environment and FPA conditions. However, in this particular experiment, the ground controls were not controlled for vibrational forces and changes in gravity including hyper, micro and 1 g forces throughout the flight. In-flight and actual temperature HUVEC-onto microcarriers were collected in 15 ml centrifuge tubes. Osmium tetroxide (2%) was added into the centrifuge tube and incubated for 1 hour at room temperature. The cells were washed with PBS 3 times. Cells were then dropped on a stub and placed in the fume hood until dried. The samples were examined under a SEM Quanta FEG 200F from FEI under low vacuum using ESEM (environmental scanning mode). Low vacuum mode enabled the operator to examine virtually any sample in the SEM without time-consuming sample preparation.

### *Fluorescent staining of revived and control HUVEC for confocal microscopy*

Upon arrival at the laboratory, the FPAs were carefully unpacked to collect HUVEC on microcarriers. HUVEC were then detached from the microcarriers using Accutase, centrifuged

**TABLE 1: Recorded temperature profile during the spaceflight travel**

Time (days)	Activities	Temperature
L (launch) + 12 hours	FPA's loading in Soyuz TMA-11	Ambient (18-28 °C)
L +1 (1 day after launch)	Launching	Ambient (18-28 °C)
L +2	Docking	Ambient
L +3	Transferring of FPA into 37°C incubator	37°C
L +4	Addition of culture medium	37°C
L +10	Termination	Ambient (28°C)
L +11	Undocking	Ambient (18-28°C)
L +12	Landing and retrieval	4°C

and transferred into a T-25 cm<sup>2</sup> culture flask containing M200 culture medium with 10% heat inactivated fetal bovine serum (FBS). Revived live endothelial cells (RAP) were passaged and cultured prior to confocal microscopy analysis. Cells were harvested and cultured in petri dishes at density of  $1.0 \times 10^5$  cells (passage 9). Cells were cultured until 80% confluency prior to cell staining. HUVEC cells at passage 9 which did not undergo spaceflight travel were used as controls (control HUVEC). The cells were washed with PBS and directly stained with Mito Tracker (CMXRos), Tubulin Tracker (Oregon Gorex 488 Taxol his-acetate) according to the manufacturer concentration recommendation with nuclei counterstained with Hoechst 33342. The cells were incubated at room temperature (20-25°C<sup>0</sup>) in the dark for 15 minutes with gentle shaking. Fluorescence-stained cells were examined under the inverted Confocal Laser Scanning Microscope (Leica TCS SP5), which was equipped with a laser confocal system, comprising a 405 Diode laser, argon laser, HeNe 543 & 633 and four photomultiplier tubes. Image processing was carried out with Leica QWin software.

#### *Cell growth analysis*

RAP and control HUVEC were cultured in medium M200 supplemented with low serum growth supplements in T-25 cm<sup>2</sup> culture flask and cultured until confluence. Cells were harvested with cell detachment solution (Accutase) and seeded in 6-well culture plates at a seeding density of  $5.7 \times 10^4$  cells per well (passage

9). In order to assess the cell viability, cells were harvested and stained with trypan blue solution (0.4%). Viable cells were counted using hemocytometer at several timelines (48, 96 and 144 hours).

#### *Digital morphometry*

RAP and control HUVEC were double-stained for mitochondria and tubulin markers and counterstained by Hoechst 33342 then photographed using a 40x objective. The captured images of cells were recorded for blind image analysis by two investigators and quantified using commercially available Leica QWin software (Leica Imaging systems, UK). The contours of the integral cells and their nuclei were outlined, images were calibrated and measurements (area, perimeter, long and short diameters) were performed. The intensity of intracellular fluorescence (RGB) for each cell (red for mitochondria and green for tubulin) was also quantified.

The measurements were transported to Excel software version 3.05 (GraphPad Software, USA) with subsequent estimation regularity index (RI) of the cells and their nuclei (estimated as  $RI = \pi * LW/4A$ ) [12], ellipticity index of the cells (estimated as  $EI = L/W$ ) [12], nucleus to cytoplasm ratio. Mean values and their standard errors were calculated. The significant differences in these parameters in normal and RAP cells were assessed by the Student's t-test. The level of significance was set at  $p < 0.05$ .

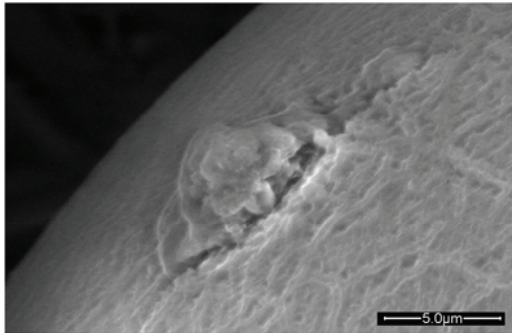


FIG. 1a. ESEM of the small control HUVEC with one process and protruding nucleus-containing part. x12,000

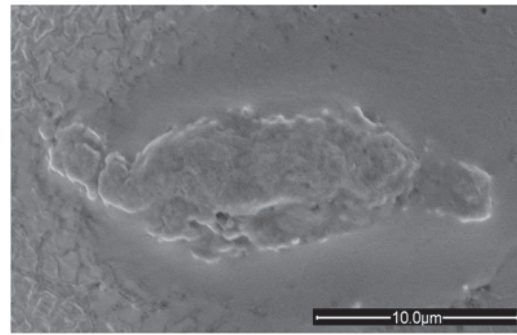


FIG. 1b. ESEM of the control HUVEC with two processes surrounded by lamelloplasm. x10,000

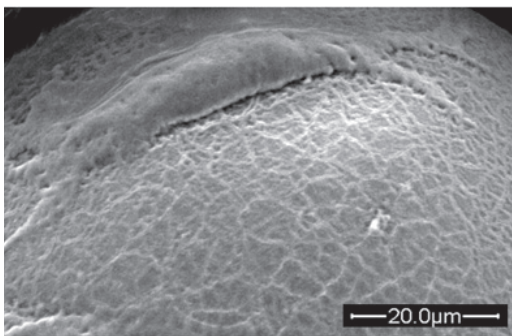


FIG. 1c. ESEM of the large spindle-shaped IPF HUVEC with the two branching processes. x4,000

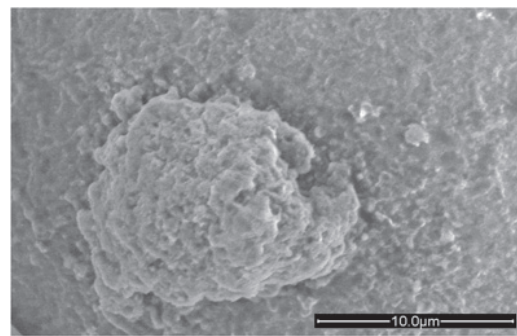


FIG. 1d. ESEM of the small round IPF HUVEC with protruding central part and the two outgrowths. x10,000

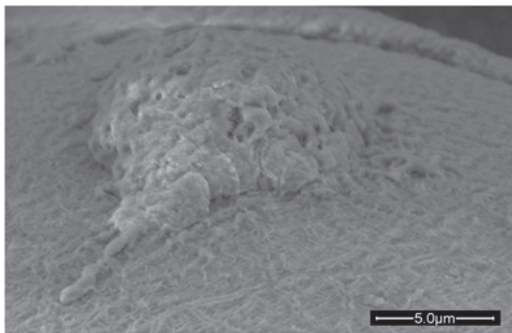


FIG. 1e. ESEM of the flattened IPF HUVEC with a single short thin process. x12,000

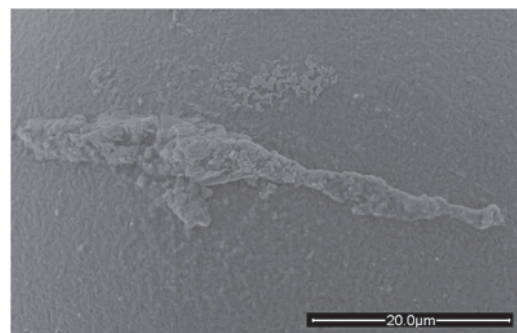


FIG. 1f. ESEM of the long slim IPF HUVEC with two processes. x5,000

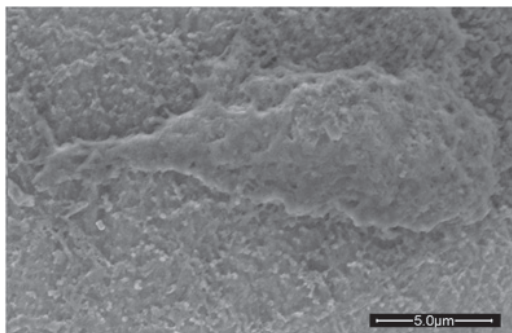


FIG. 1g. ESEM of the flattened IPF HUVEC with a single short thick process. x12,000.

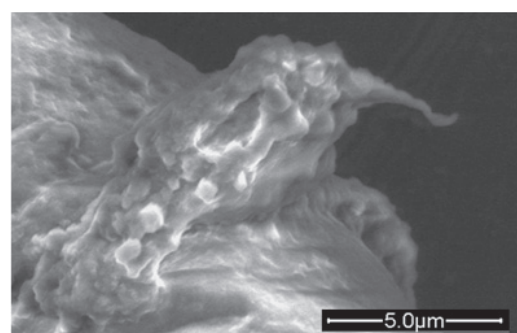


FIG. 1h. ESEM of the IPF HUVEC with numerous blebs. x12,000

## RESULTS

### *Scanning electron microscopy of control and immediate post-flight HUVEC*

SEM investigation provided some new details on the structure of the space-flown cells (Fig.1). Normal HUVEC appeared as elongated cells with rather uniform shape. Most of the cells contained a centrally located protruding nucleus, one or two tapering processes and rarely exhibited few blebs (Fig.1a,b). Some of the cells were surrounded by lamelloplasm (Fig.1b).

In contrast, IPF HUVEC (Fig.1c,d,e,f) mostly were larger in size compared to the control HUVEC (Fig.1c,d), with an irregular surface and increased number of processes and outgrowths (Fig.1c). The heterogeneity of the cell appearance: from small round cells with a diameter around 5  $\mu\text{m}$  (Fig.1d) to large cells with irregular contours more than 40  $\mu\text{m}$  long (Fig.1c,e), was also typical for the IPF culture cells. Many of them lost their typical spindle-like shape. Some of the cells contained flattened nuclei (Fig.1f,g). Many IPF HUVEC displayed an increased amount of blebs (Fig.1h).

### *Fluorescence microscopy of control and revived HUVEC*

Control HUVEC growing on a flat surface assumed an elongated spindle-shaped form with tapering processes (Fig.2a,b). Fewer cells were round or oval with one or more than two processes. In most control cells the bright red (for mitochondria) and green (for tubulin) fluorescence was rather evenly distributed in the cytoplasm, although in some HUVEC mitochondria and tubulin markers looked polarized.

Images of the RAP HUVEC differed considerably from the normal endothelial cells (Fig.2c,d). Their size and shape varied much more than in the control cells. In many cells the size of the cells was notably larger. The contours became intricate with many processes of different length and shape, including confluent ones (Fig.2d). Bundles of the tubulin-positive structures in some cells became very prominent and often occupied the periphery of the cytoplasm (Fig.2d). Staining for mitochondria in many cells appeared to be reduced (Fig.2c).

The results of the digital morphometry of the fluorescent images are shown in Figs.3 & 4. Data are expressed as mean  $\pm$  SE. As it follows from Fig.3, the morphometric parameters of RAP HUVEC, such as perimeter

and ellipticity index were significantly higher than in the control cells ( $p < 0.001$ ). They were increased compared to controls by 338% and 47% respectively. The regularity index of the RAP cells was by 23% higher ( $p < 0.05$ ) against control HUVEC, showing an increased irregularity of the cell surface compared to the normal cells. Similarly, the perimeter of the nuclei (Fig.4) was significantly (by 62%) enlarged in the RAP cells compared to the control ones ( $p < 0.001$ ). The regularity index of the nuclei did not differ significantly between normal and RAP cells. Nucleus to cytoplasm ratio in RAP cells decreased by 46% ( $p < 0.001$ ).

There was a significant decrease (Fig.5) in the intensity of the red fluorescence (staining for mitochondria) by 32% ( $p < 0.001$ ) and green fluorescence (staining for tubulin) by 18% ( $p < 0.05$ ) in the cytoplasm of RAP HUVEC compared to control cells ( $p < 0.001$ ).

### *Growth rate of the normal and revived HUVEC*

Fig.6 showed the growth rate of the HUVEC over the time period between 0-144 hours. Three samples were obtained for each timed specimen i.e. at 48, 96 and 144 hours. For each sample, the experiments were performed in triplicates ( $n=3$ ). The control HUVEC demonstrated an increment in the cell count over the time period (the cell numbers were increased when compared after 48 hours vs. 0 hours,  $p < 0.05$ ; after 96 hours vs. 48 hours,  $p < 0.05$ ; 144 hours vs. 96 hours,  $p < 0.05$ ). In contrast, the RAP cells exhibited a diminished increment in cell number over the same time period compared to normal HUVEC ( $p < 0.05$  in 48 hours vs. 0 hours; NS in 96 hours vs. 48 hours; NS in 144 hours vs. 96 hours). The cell numbers of RAP cells were markedly reduced compared to control HUVEC ( $p < 0.05$  after 48 hours,  $p < 0.001$  after 96 and 144 hours).

## DISCUSSION

Cultured endothelial cell phenotype and behavior are dramatically affected by simulated microgravity modeled by clinostat rotation or random positioning machines, as established by several investigators.<sup>1,13,4,14-16,5,17,18,6</sup> The authors showed not only functional but also morphological and transcription alterations in the endothelial cells exposed to simulated hypogravity. There are controversial reports on the growth and proliferation rate of the cells exposed to modeled microgravity. Diminished proliferative activity

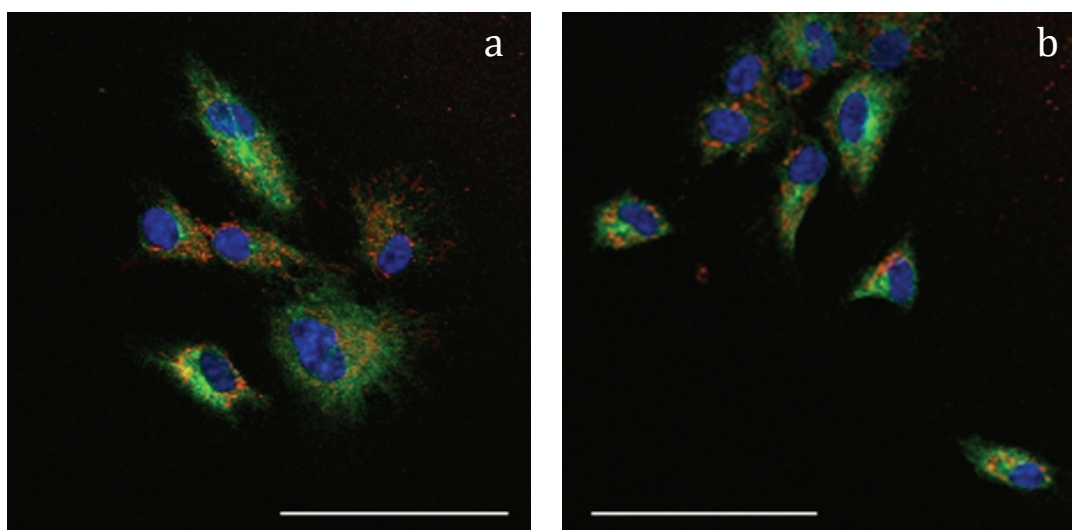


FIG. 2 (a,b). Control HUVEC, fluorescent staining for tubulin (green) and mitochondria (red); nuclei are counterstained by Hoechst 33342 (blue). Bar – 50  $\mu$ m.

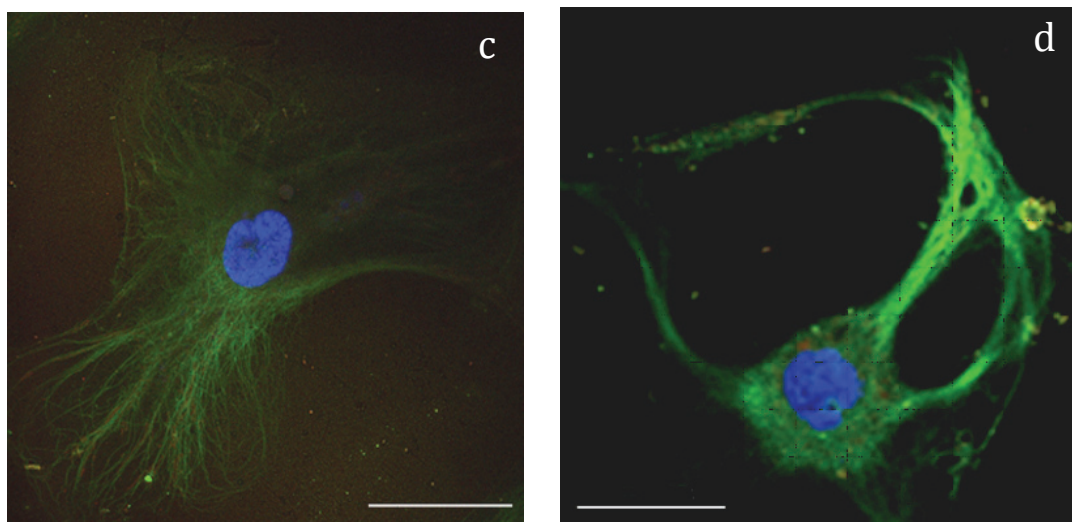


FIG. 2 (c,d). RAP HUVEC, fluorescent staining for tubulin (green) and mitochondria (red); nuclei are counterstained by Hoechst 33342 (blue). Bar 50  $\mu$ m.

in the HUVEC was reported in one of the first papers on the cultured endothelial cell under simulated microgravity<sup>1</sup> while others showed an increased growth and proliferation rate.<sup>19,17</sup> Decreased level of proliferation in porcine aortal cells after 72 hours of simulated microgravity and increased apoptotic rate was demonstrated with expression of apoptotic genes being higher in the microgravity exposed cells, while anti-apoptotic genes were up-regulated in control cells. The PCNA transcript, a marker of cell mitosis, was also found to be decreased in the absence of gravity.<sup>15</sup> Our findings on real microgravity showed that the cell growth in the RAP cells

remained lower compared to the control HUVEC. Our data on the cell growth of the RAP cells are in agreement with the data by some investigators,<sup>1</sup> but contradict the findings of others.<sup>19</sup>

The effect of microgravity on the growth and proliferation rate was showed to be dependent on the type of endothelial cells.<sup>13</sup> Under simulated microgravity, macrovascular endothelial cells proliferate faster than the control cultured cells, while microvascular endotheliocytes' proliferation is inhibited.<sup>17</sup> Similar results were obtained for microvascular 1G11 cells.<sup>14</sup> These observations are in agreement with authors<sup>20,21</sup> who demonstrated that endothelial cells from

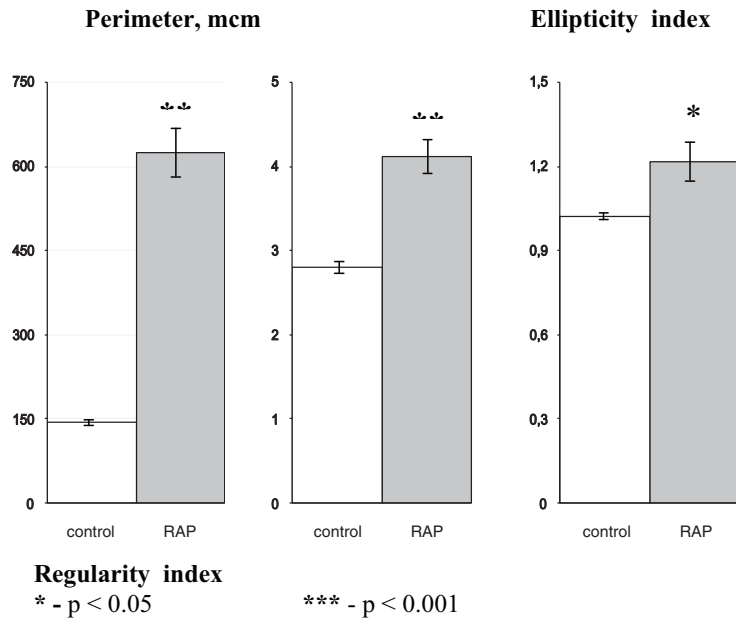


FIG. 3. Digital morphometry of the control and RAP HUVEC, (M±SE)

different segments of the vascular system showed diverse adaptational changes under microgravity and other environmental challenges. For our experiment we selected HUVEC as the most common type of endothelial cells used in the microgravity-related experiments in order to be able to compare our results obtained in real space with the data from other investigators on simulated weightlessness.

The inhibition of cell growth and p21 upregulation by simulated hypogravity were reversible upon return to normal gravity.<sup>14</sup> Analogously, HUVEC microgravity-induced dysfunctions also were shown to be rapidly reversible upon return to normal culture conditions.<sup>13</sup> Contrary to these observations, we discovered a different reaction of the RAP cells after 12-day outer space flight which was

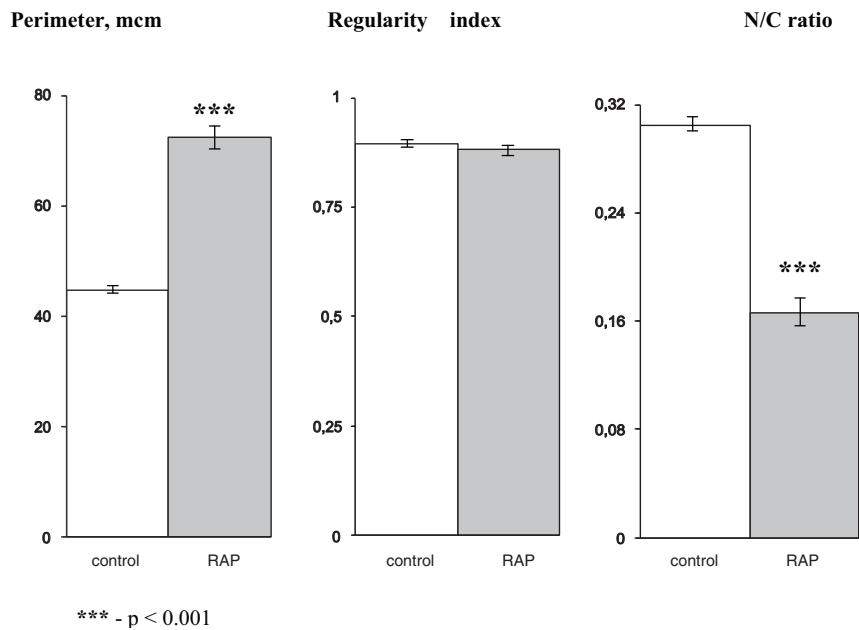


FIG. 4. Digital morphometry of the nuclei and nucleus to cytoplasm ratio of the control and RAP HUVEC(M±SE)

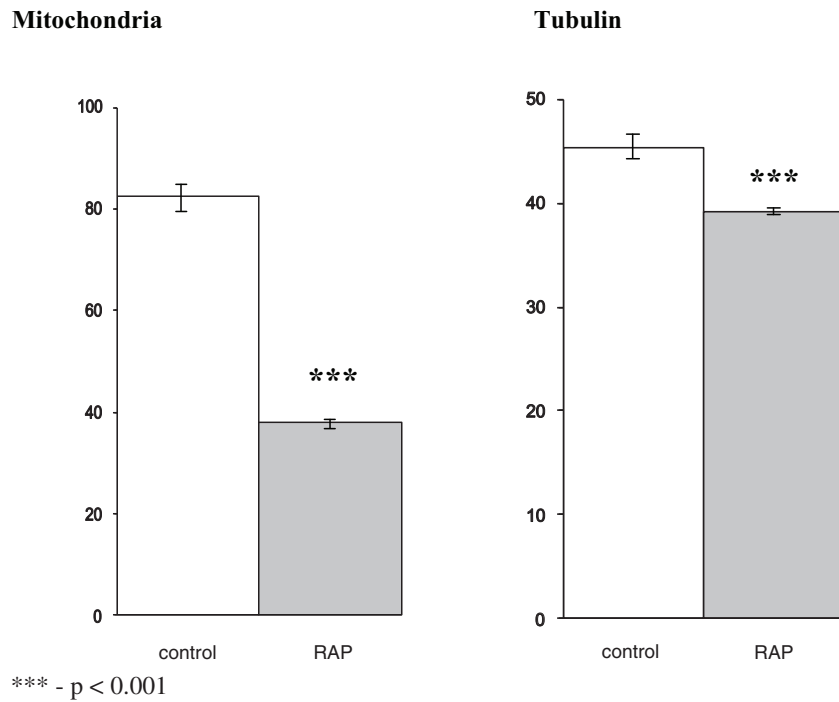


FIG. 5. Intensity of fluorescent staining (RGB) of cytoplasm of the control and RAP HUVEC(M+/-SE)

not reversible even after 9 passages. Our data obtained in real microgravity differ from the investigations on stimulated microgravity which may be explained by presence of additional factors during outer space flight, such as short-term hypergravitation. As was demonstrated earlier, even an 8 min. hypergravitation exposure may abolish the effect of microgravitation regarding cell growth and proliferation rate.<sup>5</sup>

Increased irregularity of the cell surface in the post-flight cells demonstrated in our study may be explained by cytoskeleton damage under microgravity conditions as indicated by the significantly reduced intensity of the tubulin-positive staining in the hypertrophied HUVEC. Hypertrophy of revived cells may be the mechanism accounting for the adaptation of the cells to the space conditions. It was

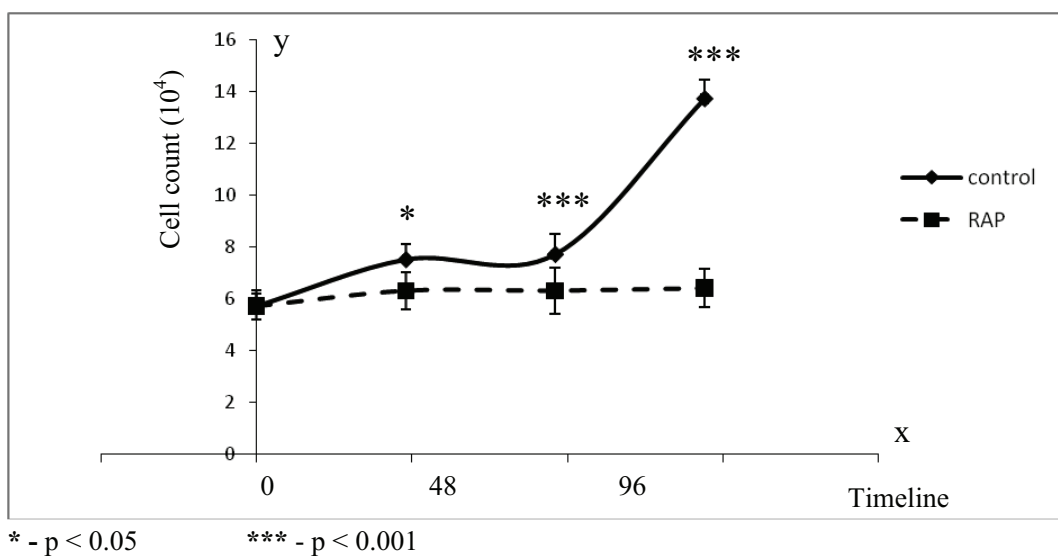


FIG. 6. Growth rate of the control and RAP HUVEC (M+/-SE)

established earlier that cell exposure to both real and simulated hypogravity conditions causes cytoskeleton disorganization associated with microtubule disruption.<sup>22,18</sup> It is known that cells exercise size homeostasis. Cytoskeleton regulates endothelial cell shape and size changes and signaling pathways essential for endothelial cell morphogenesis. Cytoskeletal disorganization results in a failure of mitochondria transport along microtubules, followed by mitochondria clustering and alterations.<sup>7</sup> Changes in the shape of the HUVEC under simulated microgravity were presumed to be associated with cytoskeletal alterations.<sup>1</sup> A few investigators demonstrated disrupted cytoskeleton and mitochondrial lesions in the cultured endothelial cells under simulated microgravity.<sup>13,4,15,23,5,18,6</sup> Among the mechanisms of cytoskeletal disruption, downregulation of actin through a transcriptional mechanism is proposed, which is considered to be an adaptive change to avoid accumulation of the redundant fibers. Recently, with the use of breast adenocarcinoma cells it was showed by immunofluorescent staining for beta-tubulin and F-actin<sup>24</sup> that modeled microgravity disorganizes cytoskeleton filaments (microfilaments and microtubules), though quantitative evaluation of the beta-tubulin and F-actin-positive structures was not presented by the authors. Recent investigation of the cultured endothelial cells during 22 sec parabolic flight microgravity revealed a cytoplasmic rearrangement of  $\beta$ -tubulin immunofluorescence suggesting that microgravity alters the gene expression patterns and the cytoskeleton of endothelial cells very early.<sup>25</sup> The changes in the size and shape of the HUVEC demonstrated in our study are typical for cytoskeleton disturbances. Our observations show cytoskeletal disruption not only in the IPF endotheliocytes but also in the RAP HUVEC.

Our quantitative analysis of the RAP cells demonstrated that the tubulin staining in their cytoplasm is decreased, which contradicts the results of another study<sup>16</sup> which showed that the tubulin staining in the endothelial cells under simulated microgravity is increased while microtubules look coiled getting in close association with the nucleus. Explanation of these findings is not given in that paper, and the quantitative analysis of these changes was not applied. In our experiment the bundles of tubulin-positive structures in some cells appeared to be thicker and brighter in the cellular processes rather than in the perinuclear region. In general,

staining was brighter in the control cells than in the postflight ones. Digital morphometry confirmed that the tubulin staining of the postflight cells was significantly lower compared to the ground control cells. A reason for the discrepancy may be microgravity exposure of another cell line by other investigators<sup>16</sup> and also the different conditions of the experiment using real and simulated hypogravity accordingly.

As it was shown by other investigators major modifications of cell shape in space were evident within 4 h. from the beginning of the experiment and remained for several days. The cells became elongated, showed extended cytopodia, and the actin fibers were disorganized and formed clusters especially in the perinuclear position. These cytoskeletal modifications were reversible upon return to normal growth conditions.<sup>13</sup> In our experiment, cytoskeletal disruption according to the image analysis data persisted in the revived cells for as many as 9 passages, which also may be explained by different conditions of stimulated and real hypogravity.

It is widely known that quiescence cells have reduced proliferation but remain metabolically active. In contrast, senescence cells are both non-proliferative and metabolically inactive. In this present study we showed that the RAP cells exhibit markedly reduced proliferation compared to controls. This suggests that the RAP cells are in the senescence stage where they have exhibited reduced cellular proliferation and metabolic activity evaluated by intensity of fluorescent staining for mitochondria. The confocal microscopy data from this present study clearly showed that the intensity of staining for mitochondria was reduced, suggesting that there was decreased metabolic activity in the RAP cells. Taking into account all these findings, we can conclude that these post real spaceflight revived endothelial cells are in the senescence state.

It is known that microgravity is not the only adverse factor of outer space flight; the others are radiation, vibration, mechanical stress and temperature changes. The control HUVEC in our research were matched for temperature profile as in the space experiment during assessment of growth rate. Our temperature control investigations demonstrated that the HUVEC exposed to the space flight factors had a slower growth rate than the ground temperature control cells. Therefore we can comment that, since temperature was controlled in our experimental groups of HUVEC and temperature fluctuations

during space flight did not show any depression of the growth rate of the HUVEC, this factor can be excluded from the list of factors contributing to the inhibited growth rate. Although microgravity may be postulated as a possible cause of reduced growth rate, other factors like radiation, vibration and physical stress cannot be excluded as possible causes contributing to the decreased growth rate in the RAP cells.

Taken together, our results demonstrate that short space flight and the post-flight (up to 3 months) period are associated with cytoskeletal lesions in the endothelial cells as indicated by SEM and confocal microscopic findings. Intricate contour changes and increased size of the IPF cells discovered by SEM are suggestive of cytoskeletal disruption. These may contribute to endothelial dysfunction possibly attributed in part to microgravity associated with space flight.

#### ACKNOWLEDGEMENTS

This investigation was sponsored by a Malaysian Ministry of Science, Technology and Innovation (MOSTI) research grant (grant code 07-01-01-SS005) awarded to the project leader Prof Hapizah Mohd Nawawi. The authors would like to thank the ANGKASA, IBMP (Moscow) and Faculty of Medicine, UiTM for all the support rendered.

#### REFERENCES

- Romanov Y, Kabaeva N, Buravkova L. Simulated hypogravity stimulates cell spreading and wound healing in cultured human vascular endothelial cells. *J Gravit Physiol.* 2000;7: 77-8.
- Romanov IuA, Kabaeva NV, Buravkova LB. Alterations in actin cytoskeleton and rate of reparation of human endothelium (the wound-healing model) under the condition of clinostatting. *Aviakosm Ekol Med.* 2001;35: 37-40.
- Buravkova LB, Romanov YA. The role of cytoskeleton in cell changes under condition of simulated microgravity. *Acta Astronaut.* 2001; 48: 647-50.
- Bradamante S, Barenghi L, Villa L. Simulated weightlessness in the design and exploitation of a NMR-compatible bioreactor. *Biotechnol Prog.* 2004; 20: 1454-9.
- Versari S, Villa A, Bradamante S, Maier JA. Alterations of the actin cytoskeleton and increased nitric oxide synthesis are common features in human primary endothelial cell response to changes in gravity. *Biochim Biophys Acta.* 2007; 1773: 1645-52.
- Griffoni C, Di Molfetta S, Fantozzi L, *et al.* Modification of proteins secreted by endothelial cells during modeled low gravity exposure. *J Cell Biochem.* 2011; 112: 265-72.
- Schatten H, Lewis ML, Chakrabarti A. Spaceflight and clinorotation cause cytoskeleton and mitochondria changes and increases in apoptosis in cultured cells. *Acta Astronaut.* 2001; 49: 399-418.
- Buravkova L, Romanov Y, Rykova M, Grigorieva O, Merzlikina N. Cell-to-cell interactions in changed gravity: ground-based and flight experiments. *Acta Astronaut.* 2005; 57: 67-74.
- Monticone M, Liu Y, Pujic N, Cancedda R. Activation of nervous system development genes in bone marrow derived mesenchymal stem cells following spaceflight exposure. *J Cell Biochem.* 2010; 111: 442-52.
- Talbot NC, Caperna TJ, Blomberg L, Graninger PG, Stodieck LS. The effects of space flight and microgravity on the growth and differentiation of PICM-19 pig liver stem cells. *In vitro Cell Dev Biol Anim.* 2010; 46: 502-15.
- Nawawi H, Osman NS, Annuar R, Khalid BA, Khalid BA, Yusoff K. Soluble intercellular adhesion molecule-1 and interleukin-6 levels reflect endothelial dysfunction in patients with primary hypercholesterolaemia treated with atorvastatin. *Atherosclerosis.* 2003; 169: 283-91.
- Saravia F, Nunez-Martinez I, Moran JM, *et al.* Differences in boar sperm headshape and dimensions recorded by computer-assisted sperm morphometry are not related to chromatin integrity. *Theriogenology* 2007; 68: 196 –203.
- Carlsson SI, Bertilaccio MT, Ballabio E, Maier EA. Endothelial stress by gravitational unloading: effects on cell growth and cytoskeletal organization. *Biochim Biophys Acta.* 2003; 1642: 173-9.
- Cotrupi S, Ranzani D, Maier JA. Impact of modeled microgravity on microvascular endothelial cells. *Biochim Biophys Acta.* 2005; 1746: 163-8.
- Morbidelli L, Monici M, Marziliano N, *et al.* Simulated hypogravity impairs the angiogenic response of endothelium by up-regulating apoptotic signals. *Biochem Biophys Res Commun.* 2005; 334: 491-9.
- Infanger M, Kossmehl P, Shakibaei M, *et al.* Induction of three-dimensional assembly and increase in apoptosis of human endothelial cells by simulated microgravity: impact of vascular endothelial growth factor. *Apoptosis.* 2006; 11: 749-64.
- Mariotti M, Maier JA. Gravitational unloading induces an anti-angiogenic phenotype in human microvascular endothelial cells. *J Cell Biochem.* 2008; 104:129-35.
- Siamwala JH., Reddy SH., Majumder S, Kolluru GK., *et al.* Simulated microgravity perturbs actin polymerization to promote nitric oxide-associated migration in human immortalized Eahy926 cells. *Protoplasma.* 2010; 242:3-12.
- Carlsson SI, Bertilaccio MT, Ascari I, Bradamante S, Maier JA. Modulation of human endothelial cell behaviour in simulated microgravity. *J Gravit Physiol.* 2002; 9: 273-4.
- Jingaa VV, Gafencua A, Antohea F, *et al.* Establishment of a pure vascular endothelial cell

- line from human placenta. *Placenta*. 2000; 21: 325–36.
21. Lang I, Pabs MA, Hiden U, *et al.* Heterogeneity of microvascular endothelial cells isolated from human term placenta and macrovascular umbilical vein endothelial cells. *Eur J Cell Biol*. 2003; 82: 163–73.
  22. Papaseit C, Pochon N, Tabony J. Microtubule self-organization is gravity-dependent. *Proc Natl Acad Sci USA*. 2000; 97: 8364-8.
  23. Infanger M, Ulbrich C, Baatout S, *et al.* Modeled gravitational unloading induced downregulation of endothelin-1 in human endothelial cells. *J Cell Biochem*. 2007; 101:1439-55.
  24. Li J, Zhang S, Chen J, Du T, Wang Y, Wang Z. Modeled microgravity causes changes in the cytoskeleton and focal adhesions, and decreases in migration in malignant human MCF-7 cells. *Protoplasma*. 2009; 238: 23–33.
  25. Grosse J, Wehland M, Pietsch J, *et al.* Short-term weightlessness produced by parabolic flight maneuvers altered gene expression patterns in human endothelial cells. *FASEB J*. 2012; 26:639-55.